Combination of photoelectrocatalysis and ozonation: A novel and powerful approach applied in Acid Yellow 1 mineralization

Guilherme Garcia Bessegato, Juliano Carvalho Cardoso, Bianca Ferreira da Silva, Maria Valnice Boldrin Zanoni *

Department of Analytical Chemistry, Institute of Chemistry, Universidade Estadual Paulista "Júlio de Mesquita Filho"—UNESP. Av. Prof. Francisco Degni, 55, 14800-060, Araraquara, SP, Brazil

ARTICLE INFO

ABSTRACT

Photoelectrocatalytic oxidation (PEC) is known to be a powerful technique employed with the aim of promoting organic degradation. Its efficiency is nonetheless found to be dramatically decreased when applied in highly concentrated effluent treatment owing to the reduced transparency which minimizes the photons reaching the semiconductor surface. In light of that, the present work seeks to describe a novel combination of photoelectrocatalysis and ozonation (O_3 + PEC) techniques, aiming at achieving a faster decolorization of a highly concentrated solution and a higher rate of mineralization. The Acid Yellow 1 dye (AY1), widely used in cosmetics was chosen as a colorful solution model. TiO_2 nanotubes electrode was used as photoanode in an annular bubble reactor operating at 2.0 V with UV-B irradiation in the presence of 1.25×10^{-4} mol min^{-1} of O_3. The main factors interfering in the O_3 + PEC process were optimized through UV/vis spectrophotometry, total organic carbon (TOC) and mass spectrometry measurements. After 20 min of treatment using the combined system, 100% of decolorization was observed while a total mineralization was seen following 60 min of treatment even in effluents containing 100 ppm AY1. Concomitantly, the combined system (O_3 + PEC) showed higher decolorization rate constant and lower energy consumption compared to the other techniques, showing that O_3 + PEC is a successful, efficient and cost-effective alternative for water treatment.

© 2015 Elsevier B.V. All rights reserved.

1. Introduction

Photoelectrocatalytic (PEC) treatment of environmental pollutants has been studied over the years [1] and great advances in this area have been reached with the progress in materials research, mainly nanostructured materials and modified/doped semiconductors [2,3]. TiO_2 is widely employed in photo(electro) catalysis due to its wide range of properties, has the ability to be prepared in various morphologies and energy position of the valence band capable of producing hydroxyl radicals. TiO_2 nanotubes (TiO_2NTs) have been the subject of many papers in various fields such as solar cells [4], water splitting [5,6], sensors [7], CO_2 reduction [8] and as a photocatalyst for the degradation of environmental contaminants [9,10]. For photo(electro)catalytic applications, the morphology of the nanotubes has been shown to be the most efficient mainly because of its large surface area and its excellent electronic transport of photogenerated charge carriers, reducing the recombination of electron/hole pair [11].

PEC treatment is embedded on the generation of hydroxyl radicals (•OH), which makes it therefore an intrinsic example of the techniques classified as advanced oxidation processes (AOPs) [3,12]. The core of this technique lies in the irradiation of a semiconductor (SC) biased by a potential gradient relatively higher than its flat band potential. The increase in band bending within the TiO_2 particles promoted electrons depletion and the enrichment of holes on the SC surface. The photogenerated electrons on the anode are then redirected to the cathode through the electrochemical system, where reduction reactions may occur [1,3,12,13]. Thus, the quantum efficiency is increased whilst charges recombination is minimized. However, the main drawback of photoelectrocatalysis lies in its low mineralization efficiency in highly concentrated and colored solutions such as dyes containing wastewater [13]. Under these conditions, much of the radiation emitted by the lamp is absorbed by the solution and does not reach the surface of the photoanode, creating few electron/hole pairs and reducing the ability of generating hydroxyl radicals.

* Corresponding author. Fax: +55 16 3322-2308.
E-mail address: boldrinv@iq.unesp.br (M.V.B. Zanoni).

To circumvent this problem, the combination of photoelectrocatalysis with other advanced oxidation processes is found to lead to high treatment efficiency, besides that, it can be said to be an alternative for the enhancement of the production of hydroxyl radicals (•OH) as well as for the attainment of mineralization of the contaminant in less time and with a higher efficiency [14]. Ozonation is a particularly interesting technique because it is not directly dependent on irradiation, and as a result of the ozone ability to attack double bonds selectively, it can contribute toward the decolorization of the reaction medium, while acting synergistically with photo(electro) catalysis [14,15].

Ozone is a powerful oxidant (2.07 V versus 2.8 V for •OH) that is used in water and wastewater treatment. Ozone can react with organic pollutants via two routes: direct molecular ozone oxidation reaction, which is selective and relatively slow; and/or indirect pathway where •OH radicals are produced by ozone decomposition, known to be the fastest and non-selective oxidative way (called catalytic ozonation), which is also an AOP. Ozone decomposition is dependent on pH, catalysts and UV irradiation and usually promotes the formation of more recalcitrant compounds in the end of the treatment [14,16].

The literature shows various works with the combination of heterogeneous photocatalysis with ozonation (O_3 + PC) [14,15,17,18]. It is a consensus that ozonation followed by photocatalysis is not as efficient as the two techniques operating simultaneously. However, to our best knowledge, there is no work dealing with simultaneous combination of ozonation with photoelectrocatalysis (O_3 + PEC). In this context, the present study describes a new annular bubble photoelectrocatalytic reactor combining ozonation and, photoelectrocatalytic oxidation on TiO_2NTs photoanode operating under a bias potential with UV irradiation. Acid Yellow 1 dye was used as a model compound of colorful solution, while the efficiency of the proposed method (O_3 + PEC) was compared with other systems efficiency (O_3, O_3 + UV, O3 + PC, PEC, PC and UV) and with the optimization of some parameters such as pH, voltage, flow of ozone, dye concentration and irradiation source.

2. Experimental

2.1. TiO₂ nanotube arrays electrode preparation

Photoelectrocatalytic (PEC) experiments were performed using a cylindrical TiO_2 nanotube arrays electrode (TiO_2NT), with 600 cm², with a lateral opening for solution flow. The TiO_2NT was prepared according to the methodology already published previously [10]. Ti sheet was polished using silicon carbide sandpaper of successively finer roughness and cleaned with acetone, isopropanol and finally ultrapure water. The titanium foil was shaped for cylindrical form and TiO_2 nanotubes were grown by electrochemical anodization (30 V for 50 h) using Minipa MPL-1303 power supply) in an organic electrolyte comprised of 0.25% ammonium fluoride (98%, Synth) in glycerol (99.5%, Synth) containing 10% volume Milli-Q water. The TiO_2NT electrode was cleaned in pure water, dried in N_2 and annealed at 450 °C for 30 min using heating rates of 2 °C min⁻¹. The prepared TiO_2NT was characterized by X-ray diffraction (XRD) on a SIEMENS D5000, DIFFRAC PLUS XRD Commander X-ray diffractometer with Cu-Kα radiation. The morphological characterization was carried out by field emission gun-scanning electron microscopy (FEG-SEM) on a JEOL 7500F Microscope.

2.2. Annular bubble reactor

The experiments were performed in an annular bubble reactor (ABR) with 63.5 mm diameter, 1 L of capacity and sintered glass bubblers at the bottom for injecting O_2/O_3. A Pyrex glass tube was positioned at the center of ABR where a UV-B narrowband 36 W lamp (Philips) or UV-C 36 W lamp (Osram) was positioned. For PEC experiments, the TiO_2NT electrode was placed around the glass tube and a graphite rod (diameter of 1.0 cm) was used as cathode. The bias voltage was controlled using Minipa PL-1303 power supply.

Ozone was produced by an O3R® Ozonator model ID-05 (Santa Catarina, Brazil) with a maximum capacity of 5 g O_3/h. The amount of ozone generated was determined by using an ozone analyzer ANSEROS GM-OEM in 254 nm. The input O_2 flow rate was monitored with a Cole-Parmer flowmeter (0.4–5.0 LPM). In the experiments performed without O_3 production, O_2 was bubbled in the same flow to provide the mass transport. All the experiments were performed in an isolated laboratory and inside a fume cupboard with excellent exhaustion.

2.3. Acid Yellow 1 degradation

The Acid Yellow 1 dye (AY1) degradation was carried out using initial concentration of 100 mg L⁻¹ in Na_2SO_4 0.01 mol L⁻¹ with pH 6.5. The dye was directly dissolved in deionized water. Acid Yellow 1 degradation was monitored removing aliquots at controlled times, which were analyzed by UV/vis spectrophotometry (Hewlett-Packard 8453 spectrophotometer), total organic carbon analyzer (TOC-V_{CPN}, Shimadzu) and mass spectrometry.

Different degradations were compared: photoelectrocatalytic oxidation (PEC), photocatalytic oxidation (PC), direct photolysis (UV), ozonation (O_3), ozonation + UV irradiation (O_3 + UV), ozonation + photocatalysis (O_3 + PC) and ozonation + photoelectrocatalysis (O_3 + PEC).

3. Results and discussion

3.1. Characteristics of TiO₂NT electrode

The TiO_2NT sample prepared by electrochemical anodization was characterized by X-ray diffraction (XRD) in order to confirm the TiO_2 phase formed after annealing. Fig. 1A shows the X-ray diffractogram where the peaks are indexed to the anatase phase formed after annealing the TiO_2NT. It is noteworthy that the formation of anatase phase is desirable once it exhibits a higher charge carrier mobility compared to the rutile [11], thereby contributing toward the minimization of the charges recombination. The morphological characterization was carried out by FEG–SEM and Fig. 1B shows the formation of self-aligned and self-organized nanotubes perpendicularly to the metallic substrate. The TiO_2 nanotubes presented an average diameter of 100 nm and tube wall of 11 nm.

3.2. Degradation of Acid Yellow 1 hair dye

Fig. 2A shows a representative spectrum obtained for 100 ppm of AY1 in 0.01 mol L⁻¹ Na_2SO_4 at pH 6.5 before (Curve a) and after (Curves b–i) photoelectrocatalytic oxidation conducted with the applied voltage of +2.0 V on TiO_2NT anode and graphite cathodes, using irradiation from a UV-B lamp of 36 W concomitant to an ozone flow of 1.25×10^{-4} mol min⁻¹.

A gradual reduction of absorbance is observed for all the peaks at 205 nm and 257 nm in the UV region which were attributed to the aromatics groups while 393 and 430 nm were attributed to the chromophore groups. Graphs of Fig. 2B illustrate the decolorization observed at 430 nm. As compared in Fig. 2B, the color removal is 100% after 30 min of O_3 + PEC treatment. Nevertheless, a similar behavior was obtained for the ozonation process (Fig. 2B), indicating that the fast oxidation in both processes promotes similar decolorization. However, when the TOC removal is compared
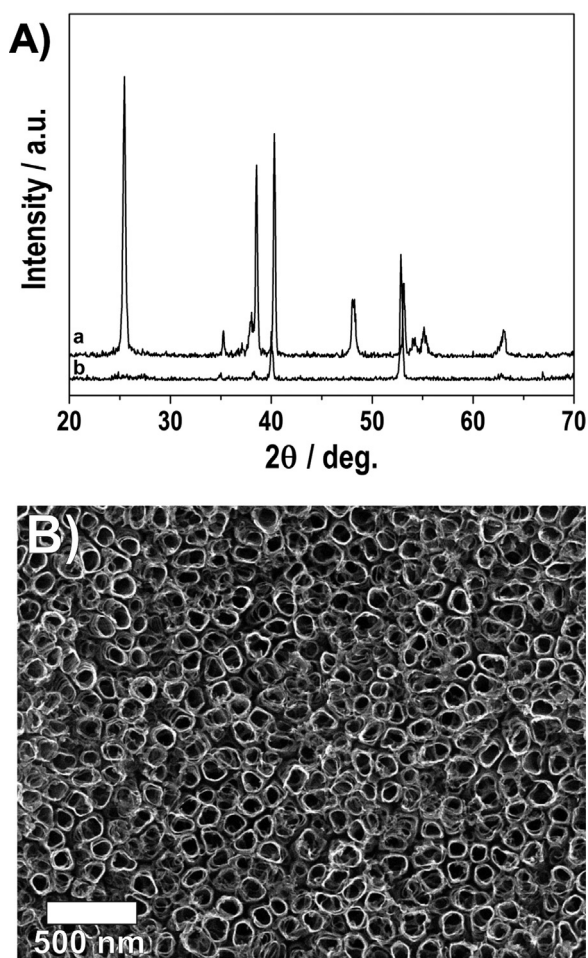
Fig. 1. (A) X-ray diffractrogram of (a) annealed TiO₂NTs sample and (b) prior to annealing TiO₂ sample and (B) FEG-SEM top view image of TiO₂ nanotubes electrode.
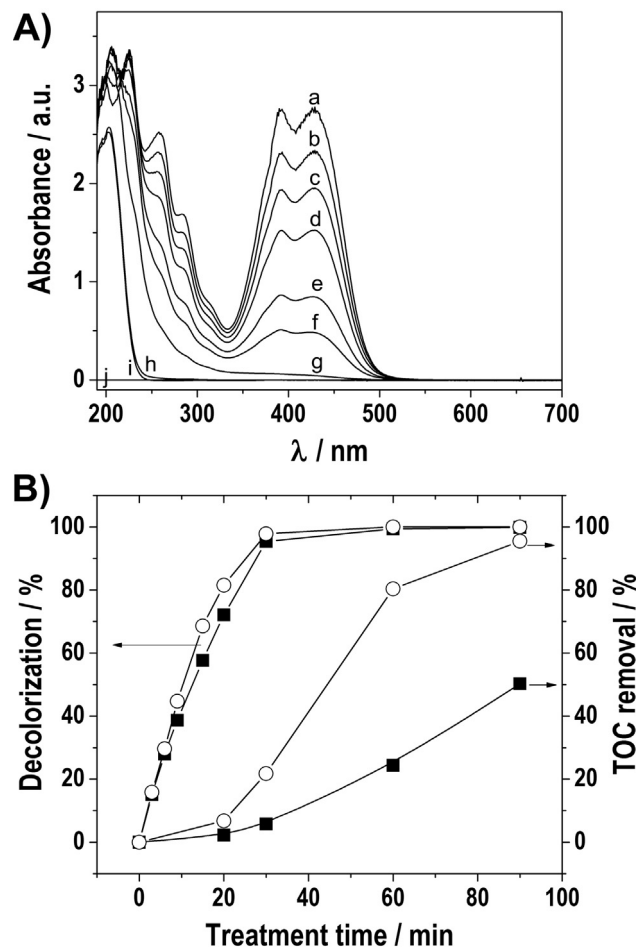

Fig. 2. (A) Representative spectrum of 100 ppm AY1 dye during O_3 + PEC treatment for (a) 0 min; (b) 3 min; (c) 6 min; (d) 9 min; (e) 15 min; (f) 20 min; (g) 30 min; (h) 60 min; (i) 90 min and (j) blank; and (B) Decolorization (%) and TOC removal (%) of 100 ppm AY1 dye during (○) O_3 + PEC and (■) O_3 treatment. Conditions: 100 mg L⁻¹ AY1 dye in 0.01 M Na₂SO₄, pH 6.5, O_3 flow of 1.25×10^{-4} mol min⁻¹; V_{app} = 2.0 V, UV-B 36 W lamp.

(Fig. 2B), it is clear that the mineralization is found to be around 4 times higher compared to the O_3 + PEC system following 60 min of treatment. This shows that the combination of these two techniques is an efficient way to increase the degradation rate of Acid Yellow 1, due to the enhanced •OH generation formed by photoelectrocatalysis and photocatalytic decomposition of ozone [14].

In order to improve the degradation efficiency using the proposed method (O_3 + PEC), the degradation of AY1 was investigated testing the effect of the pH range (3, 6.5 and 9); applied voltage (0.5 V, 2.0 V and 4.0 V) and UV lamp emitting in UV-B and UV-C region.
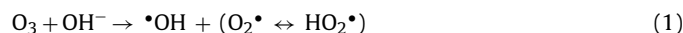
3.2.1. Effect of pH

The influence of pH (3, 6.5 and 9) in the oxidation of 100 mg L⁻¹ AY1 dye in Na₂SO₄ 0.01 M was determined by using a O_3 flow of 1.25×10^{-4} mol min⁻¹ and the TiO₂NTs operating at 2.0 V under UV-B 36 W irradiation. After 90 min of treatment, the decolorization is found to be 100% in all the investigated pH when AY1 is treated by O_3 or O_3 + PEC. The total decolorization time was 30 min for all the studied pHs using the ozonation treatment. In O_3 + PEC system, at pH 3, total decolorization is reached following 20 min of treatment and 30 min is required at pH 6.5 and 9 (data not shown). Nevertheless, the total organic carbon (TOC) removal for the ozonation process (Fig. 3A) and ozonation combined with photoelectrocatalysis (O_3 + PEC) are very different as shown in Fig. 3.

Using pure ozonation (Fig. 3A) pH 6.5 and 9 promoted a slightly better performance in TOC removal compared to pH 3. This can be explained because the catalytic ozonation process (ozone con-

version to hydroxyl radicals) is dependent on a slightly alkaline medium (Eq. (1)), which can attack the organic molecules via indirect oxidation process, as shown in Eq. (2) (where Rox represents an oxidized product) [14,15]. At an acidic pH, the ozone directly attacks the molecules (called ozonolysis) especially C=C double bonds resulting in the formation of carboxylic acids which can be recalcitrant in relation to the ozone action [14] (Eq. (3)).
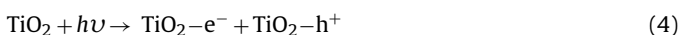
$$O_3 + OH^- \rightarrow {}^\bullet OH + (O_2^\bullet \leftrightarrow HO_2^\bullet) \tag{1}$$

$$^\bullet OH + R^\bullet \rightarrow Rox \tag{2}$$

$$O_3 + R \rightarrow Rox \tag{3}$$

When the O_3 + PEC system are tested, the maximum efficiency occurs at an acidic pH. This is also the optimum condition for PEC oxidation, where the target dye is adsorbed on the electrode surface via electrostatic interaction. Considering that the zero charge of TiO₂ presents pH$_{pzc}$ around 5.3 and the pK_a for sulphonated dyes occurs around 2.0, maximum adsorption could be occurring in acid medium when TiO₂ is positively charged [9,19].

Moreover, under the combined process of O_3 + PEC, there is the photocatalytic decomposition of ozone (to form hydroxyl radicals) (Eqs. (4–7)). The photogenerated electron on TiO₂ conduction band (CB) (Eq. (4)) can also react with the ozone generating ozonide radicals ($O_3^{\bullet-}$) (Eq. (5)). The photocatalytic decomposition of ozone is dependent on the pH, because ozonide radicals react with H⁺ in the
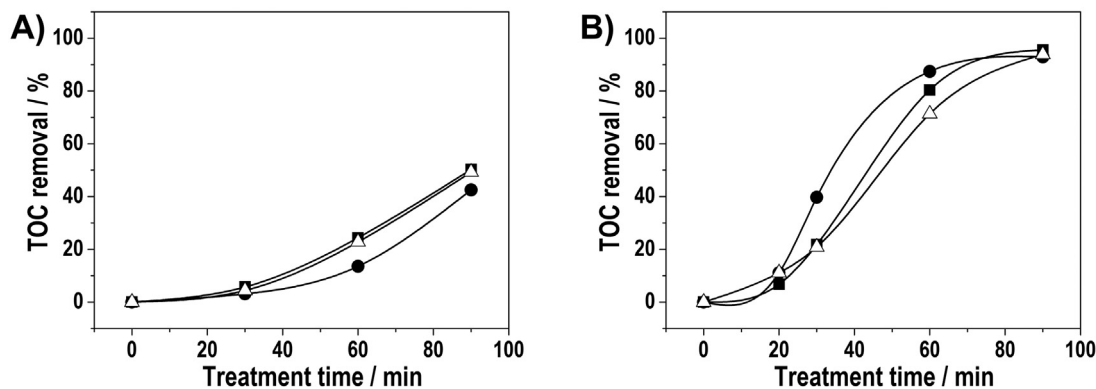
Fig. 3. Effect of pH in TOC removal for (A) ozonation and (B) ozonation combined with photoelectrocatalysis: ($\triangle$) pH 9; ($\bullet$) pH 3; ($\blacksquare$) pH 6.5. Conditions: 100 mg L^{-1} AY1 dye in Na$_2$SO$_4$ 0.01 M, O$_3$ flow of 1.25×10^{-4} mol min^{-1}, V_{app} = 2.0 V, UV-B 36 W lamp.

solution to produce HO$_3$$^\bullet$ radicals (Eq. (6)), which decomposes in OH$^\bullet$ (Eq. (7)) [14,15]:

$$TiO_2 + h\upsilon \rightarrow TiO_2 - e^- + TiO_2 - h^+ \tag{4}$$

$$O_3 + TiO_2 - e^- \rightarrow O_3^{\bullet -} \tag{5}$$

$$O_3^{\bullet -} + H^+ \rightarrow HO_3^\bullet \tag{6}$$

$$HO_3^\bullet \rightarrow O_2 + OH^\bullet \tag{7}$$

In addition, the hydroxyl radical can be produced by ultraviolet irradiation of dissolved ozone according to the following reactions [14,20]:

$$O_3 + H_2O + h\upsilon \rightarrow H_2O_2 + O_2 \tag{8}$$

$$H_2O_2 + h\upsilon \rightarrow 2OH^\bullet \tag{9}$$

$$H_2O_2 \leftrightarrow HO_2^- + H^+ \tag{10}$$

$$O_3 + HO_2^- \rightarrow O_3^{\bullet -} + HO_2^\bullet \tag{11}$$

$$HO_2^\bullet \rightarrow O_2^{\bullet -} + H^+ \tag{12}$$

$$O_3 + O_2^{\bullet -} \rightarrow O_3^{\bullet -} + O_2 \tag{13}$$

$$O_3^{\bullet -} + H^+ \leftrightarrow HO_3^\bullet \tag{14}$$
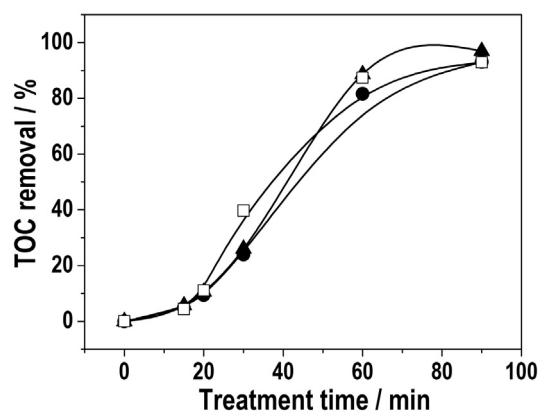
According to the above mechanism, ozonide radicals are generated (Eq. (13)), which under acidic conditions can produce hydroxyl radicals (Eqs. (6) and (7)) responsible for the mineralization of the AY1 dye.

Thus, the acidic medium increases the AY1 dye degradation rate in the O$_3$ + PEC process. Another important feature of this system has to do with the ozone contribution in overcoming the underlying demerit of photoelectrocatalysis operating in high concentrated solutions which tend to decrease the amount of light reaching the photoanode. The direct ozone attack decreases the color of the reaction medium with the formation of colorless intermediates, collaborating toward the synergistic reaction between the two processes.

3.2.2. Effect of applied voltage

In a photoelectrocatalytic process, the applied voltage is directly related to the band bending and the improvement of the charges separation [3,21]. Fig. 4 shows the effect of applied voltage in the performance of TOC removal during O$_3$ + PEC treatment. There is no significant improvement in mineralization when the different applied voltages are evaluated. This behavior is observed owing to the fact that all the applied voltages were found to be greater than the flat band potential of TiO$_2$ (E_{fb} around −0.15 V), indeed greater enough to cause a complete band bending, promoting a more efficient separation of the photogenerated electrons and holes

Fig. 4. Effect of applied potential in the TOC removal (%) during O$_3$ + PEC treatment: ($\bullet$) 0.5 V; ($\square$) 2.0 V; ($\blacktriangle$) 4.0 V. Conditions: 100 mg L^{-1} AY1 dye in 0.01 M Na$_2$SO$_4$, pH 3, O$_3$ flow of 1.25×10^{-4} mol min^{-1}, UV-B 36 W lamp.
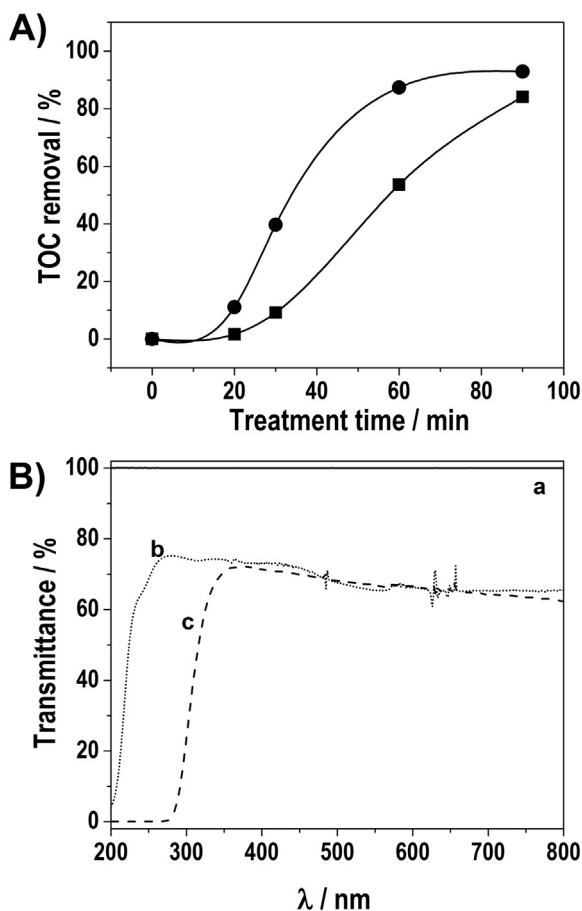
[3]. Remarkably though, a high bias potential was avoided aiming at minimizing the oxygen evolution during the photoelectrocatalytic process and a voltage of +2.0 V was chosen in further experiments.

3.2.3. Effect of lamp emission

The influence of UV irradiation on the O$_3$ + PEC treatment was evaluated using two sources: (i) a UV-B 36 W lamp with emission between 305 and 315 nm with a peak of 311 nm; and ii) UV-C 36 W lamp with emission peak of 254 nm. Fig. 5 shows the influence of these UV lamps in TOC removal (%) of 100 mg L^{-1} AY1 dye in Na$_2$SO$_4$ 0.01 M pH 3 treated for 90 min (O$_3$ flow of 1.25×10^{-4} mol min^{-1} and the TiO$_2$ NTs and bias potential of 2.0 V). It is worth pointing out the clear diminishing that can be seen in the degradation efficiency of the O$_3$ + PEC system when the photoanode is irradiated by UV-C lamp. This outcome can be said to be due to the absorption of wavelengths shorter than 300 nm by the borosilicate glass, as can be seen in Fig. 5B. Thus, smaller quantities of photons from UV-C lamp are able to reach the TiO$_2$ NTs electrode, consequently decreasing the formation of hydroxyl radicals. These results indicate that hydroxyl radicals formation still plays an essentially important role in the system.

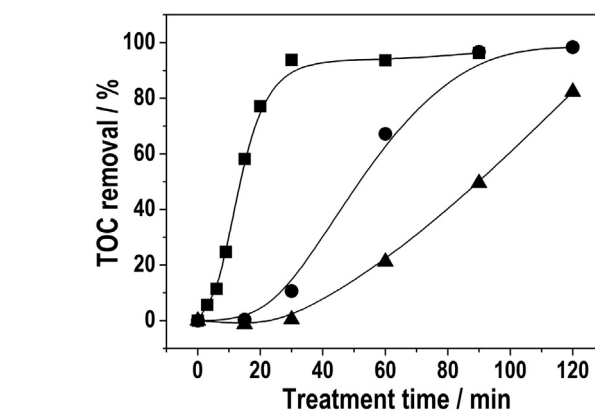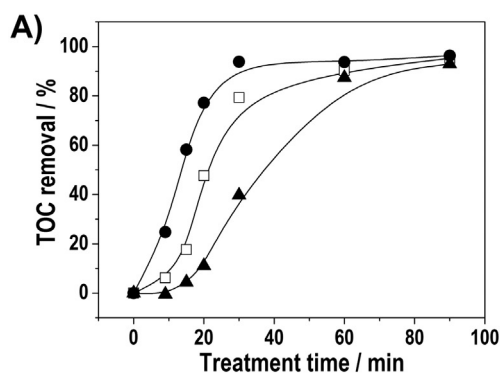### 3.2.4. Effect of O$_3$ concentration

Clearly enough, it is expected that the increasing ozone flow results in fast degradation. The performance of TOC removal was evaluated testing three different flows of ozone 1.25×10^{-4}, 3.85×10^{-4} and 6.35×10^{-4} mol O$_3$ min^{-1} (equivalent to 0.36, 1.11 and 1.83 g O$_3$/h, respectively). The decolorization was found to reach 100% in all the investigated system (data not shown). Fig. 6

Fig. 7. Effect of initial concentration of AY1 on the mineralization efficiency for O_3 + PEC treatment: (▲) 1000 ppm; (●) 500 ppm and (■ 100 ppm. Conditions: AY1 dye in 0.01 M Na_2SO_4, pH 3, O_3 flow of 6.35×10^{-4} mol min^{-1}, V_{app} = 2.0 V, UV-B lamp.

is seen to lead to an improvement in the light absorption of the photoanode.

The degradation rate is decreased in pure ozonation, as shown in Fig. 6B. The increased flow of ozone accelerates the rate of TOC removal, but the maximum mineralization is limited to ≈50%. As aforementioned, the mechanism of degradation using only the O_3 system occurs through the direct reaction of ozone whose predominance of reaction is by a selective attack resulting in non-reactive products of degradation.
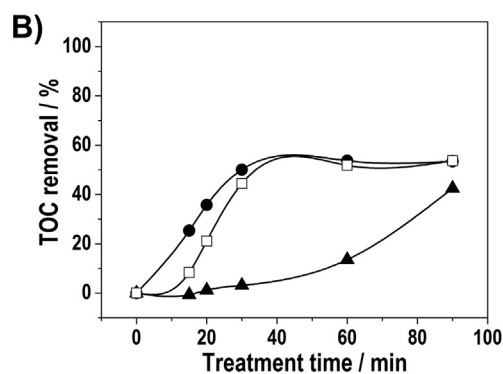
3.2.5. Effect of Acid Yellow 1 initial concentration

Fig. 7 shows the effect of the dye concentration (100, 500 and 1000 ppm) in 0.01 M Na_2SO_4, pH 3 using O_3 flow of 6.35×10^{-4} mol min^{-1}, applied potential of 2.0 V and UV-B lamp in the O_3 + PEC oxidation. An increase in the concentration from 100 ppm to 500 ppm leads to an increase in the degradation time necessary to reach total mineralization from 30 min to 90 min, and as already expected, increasing the concentration triggers a reduction in the degradation rate. These effects can be explained on grounds of the decrease in the light intensity that reaches the TiO_2 surface due to the diminishing transparency of the solution into a more concentrated solution (from 5 up to 10 times more).
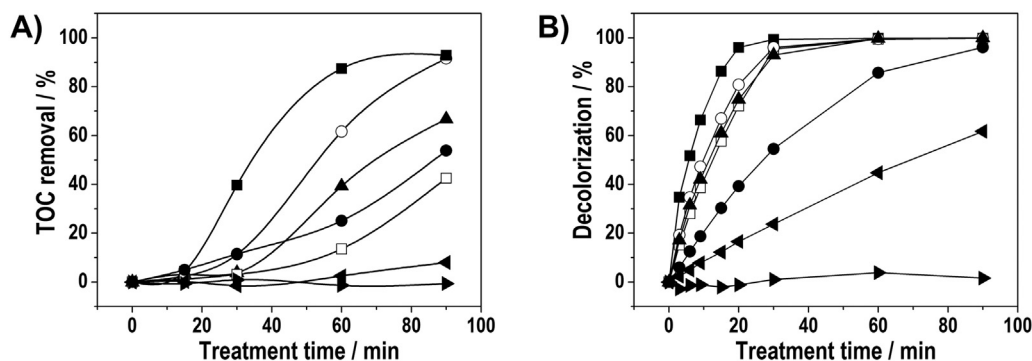
The results indicate that even at a concentration so high as 1000 ppm it is possible to achieve complete decolorization and up to 80% of mineralization within 120 min.

3.2.6. Effect of ozonation, photoelectrocatalysis, photocatalysis and combined systems on dye degradation

In order to prove the superior performance of O_3 + PEC system in relation to O_3 (ozonation), O_3 + UV (ozonation and UV

Fig. 5. (A) Effect of UV lamps on the mineralization efficiency for O_3 + PEC treatment: (●) UV-B lamp and (■) UV-C lamp. Conditions: 100 mg L^{-1} AY1 dye in 0.01 M Na_2SO_4, pH 3, O_3 flow of 1.25×10^{-4} mol min^{-1}, V_{app} = 2.0 V. (B) Transmittance (%) of: (a) air; (b) quartz and (c) borosilicate glass used in the experiments.

shows the influence of O_3 flow in O_3 + PEC treatment (Fig. 6A) and in pure ozonation (Fig. 6B). The results illustrate that the combined process clearly exerts a critically decisive role when it comes to the improvement of the dye mineralization.

During the O_3 + PEC treatment (Fig. 6A), one can notice that increasing the ozone flow results in higher mineralization rates, reaching almost complete mineralization following 30 min of treatment. This is undoubtedly a reflex of the increased amount of hydroxyl radicals being formed by the photocatalytic decomposition of ozone. In addition, the faster decolorization of the dye

Fig. 6. Effect of ozone flow in the mineralization of AY1 dye for (A) O_3 + PEC treatment and (B) O_3 treatment: (▲) 1.25×10^{-4}; (□) 3.85×10^{-4} and (●) 6.35×10^{-4} mol O_3 min^{-1}. Conditions: 100 mg L^{-1} AY1 dye in Na_2SO_4 0.01 M, pH 3, UV-B 36 W lamp and V_{app} = 2.0 V.

Fig. 8. Comparison of the degradation of AY1 dye by the different techniques (A) percentage of TOC removal of AY1 in the degradation and (B) percentage of AY1 decolorization monitored at 393 nm: (■) O_3 + PEC; (○) O_3 + PC; (▲) O_3 + UV; (●) PEC; (□) O_3; (◄) PC and () UV. Conditions: 100 ppm of AY1 in 0.01 M Na_2SO_4, pH 3, O_3 flow of 1.25×10^{-4} mol min^{-1}, UV-B 36 W lamp and V_{app} = 2.0 V.

Table 1
Decolorization rate constant (k) obtained for $\ln[A/A_0]$ versus time plot during degradation of 100 mg L^{-1} AY1 dye in 0.01 mol L^{-1} Na_2SO_4 at pH 3; UV-B 36 W lamp and V_{app} = +2.0 V under different systems.

Treatment system	k/(min^{-1})	R^2
PC	−0.0090	0.9989
PEC	−0.0250	0.9983
O_3	−0.0627	0.9924
O_3 + UV	−0.0676	0.9947
O_3 + PC	−0.0811	0.9924
O_3 + PEC	−0.1558	0.9751

irradiation), O_3 + PC (ozonation and photocatalysis using TiO$_2$NT without applied voltage), PEC (photoelectrocatalysis using TiO$_2$NT), PC (photocatalysis using TiO$_2$NT without applied voltage) and UV (direct photolysis with UV irradiation) the decolorization and mineralization of 100 ppm of AY1 were monitored during 90 min in 0.01 M Na$_2$SO$_4$, pH 3, using O$_3$ flow of 1.25×10^{-4} mol min^{-1}, UV-B 36 W lamp and V_{app} = 2.0 V for the studied systems. The results are shown in Fig. 8.

The results indicate that the combination of photoelectrocatalysis and ozonation is much more efficient compared to the O_3 + PC as the former leads to a relatively much faster decolorization and mineralization. Some works have proven that the combination of O_3 + PC results in a synergistic effect and have shown such a combination to be an efficient way of degrading organic pollutants [14,15,22–24]. Nevertheless, by a simple application of a voltage using a power supply it is possible to reach mineralization of about 90% in 60 min of treatment, while in O_3 + PC the TOC removal is 60% at the same time (a gain of about 1.4 times). Moreover, O_3 + PEC provides not only a sum of isolated O_3 and PEC processes, but it is a synergistic process.

It can also be observed that treatments based on ozonation (O_3, O_3 + UV, O_3 + PC e O_3 + PEC) result in rapid decolorization. However, O_3 treatment results in low mineralization, as seen in Fig. 8B. In O_3 + UV treatment, a relatively higher TOC removal (%) is seen compared to that observed in pure ozonation as a result of the generation of hydroxyl radicals, shown in Eqs. (5–7).

The decolorization kinetics follows a pseudo-first-order reaction (Langmuir–Hinshelwood kinetics) and the obtained constant rates of decolorization under the different systems are presented in Table 1. As can be observed, the O_3 + PEC system has a rate constant almost 2 times higher than the O_3 + PC system, which is in accord with the results shown in Fig. 8 indicating that this novel combination of photoelectrocatalysis and ozonation can considerably improve the results of photocatalytic ozonation which has already been well-established in the literature [14].

3.3. Energy consumption

For the purpose of choosing the best method for wastewater treatment, some significant factors ought to be taken under consideration including economics, effluent quality goals, regulations, operation, among others. However, economics is often the most relevant factor considered in this case and as we know AOPs are electric-energy-intensive, hence electric energy can represent the main operating cost [25,26]. Bolton et al. [25] have established standard figures-of-merit for the comparison of energy consumption independent of the nature of the system. The electrical energy per order (E_{EO}, kWh/m^3/order) is the electric energy in kilowatt hours [kWh] required to degrade a contaminant by one order of magnitude in a unit volume (1 m^3) (Eq. (15)) and it is used when the concentration of contaminant is low where the degradation follows a first-order kinetics.

$$E_{EO} = \frac{P \times t \times 1000}{V \times \log \frac{(AY1_i)}{(AY1_f)}} \tag{15}$$

Where P stands for the rated power (kW) of the oxidation system, t being the treatment time (h), V the treated volume (1 L) and AY1$_i$ and AY1$_f$ the initial and final AY1 dye concentrations after the t treatment time. The rated power is known to be equal to the sum of the individual energy consumption (EC) of the ozonator, the lamp and the power supply. The consumption of each equipment (in Wh) was calculated measuring consumed current and the utility voltage during operation with a multimeter (Minipa ET-2042D). The lamp consumes 36 Wh, the power supply consumes 8.7 Wh and the ozonator consumes 54.5, 58.9 and 67.6 Wh when it is producing 1.25×10^{-4}, 3.85×10^{-4} and 6.35×10^{-4} mol O$_3$/min, respectively.

Taking 9 min as the treatment time for the calculation of E_{EO}, Table 2 shows the E_{EO} values for the different system studied. Comparing the different systems, O_3 + PEC showed the lowest E_{EO}, for a fixed ozone flow. This indicates that the combination of ozonation and photoelectrocatalysis is the best treatment system both in respect to cost and degradation rate of AY1 dye. These results also indicate that increasing the ozone flow in O_3 + PEC from 1.25×10^{-4} to 3.85×10^{-4} and 6.35×10^{-4} mol O$_3$/min, the E_{EO} is decreased substantially from 31.5 to 10.5 and 6.6 kWh/m^3/order, respectively, indicating best values of efficiency (consumption/removal ratio). The great advantage of the O_3 + PEC relative to the O_3 + PC system lies in the applied potential which dramatically increases the efficiency of degradation (due to better separation of charges in the semiconductor and the improved catalytic conversion of O_3). As the power supply has a relatively small energy consumption and leads to a large improvement of % degradation, the O_3 + PEC system is undoubtedly expected to present a lower specific energy consumption as compared to the O_3 + PC and the other systems.

Table 2
Electrical energy per order for AY1 degradation using different systems. 100 ppm of AY1 in 0.01 M Na_2SO_4, pH 3, UV-B 36 W lamp and V_{app} = 2.0 V.

Treatment system	Ozone flow (mol min^{-1})	AY1 degradation (%) in 9 min	Electrical energy per order (kWh/m^3/order) in 9 min
PC	–	7.8	152.3
PEC	–	18.7	74.7
O_3	1.25×10^{-4}	38.7	38.5
O_3 + UV	1.25×10^{-4}	42.1	57.2
O_3 + PC	1.25×10^{-4}	47.2	48.9
O_3 + PEC	1.25×10^{-4}	66.3	31.5
O_3 + PEC	3.85×10^{-4}	96.7	10.5
O_3 + PEC	6.35×10^{-4}	99.4	6.6
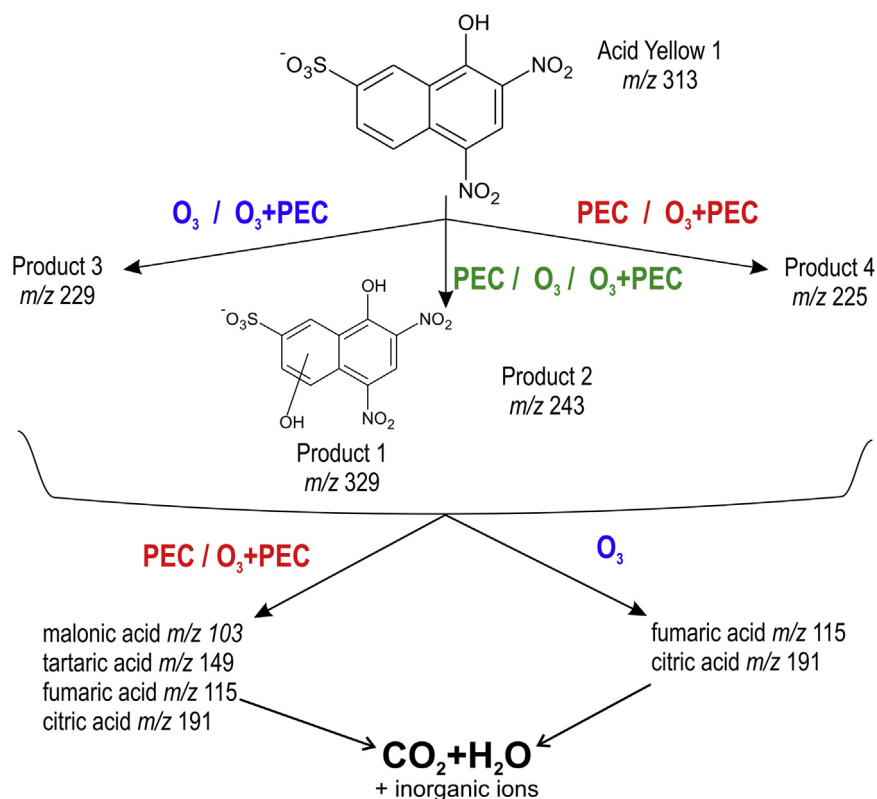
Scheme 1. AY1 dye proposed degradation pathway by different degradation processes.

Nevertheless, this calculation does not consider the system's efficiency in the dye mineralization. Although pure ozonation is said to be efficient in the removal of AY1 dye and has shown to be the second lowest E_{EO} value, it has not been possible to achieve TOC removal above 50% in this system.

3.4. Degradation intermediates of Acid Yellow 1 by LC–MS/MS analysis

It is known that during the degradation of organic compounds by AOPs various byproducts can be formed. In this context, aromatic and aliphatic intermediates formed during the AY1 degradation solutions were identified by LC–MS/MS.

The identification of the target AY1 dye and its main degradation products revealed by m/z transition detected in the negative mode was obtained by LightSight® software. The software data compared all the samples directly before subtracting them from the control or initial experiment sample. The results showed without any doubts the main difference between the chromatograms and the products formed. After analyzing all the experiments through LightSight®, including the optimized MRM and fullscan experiments, four main products were detected. The products detected were: **1** (m/z 329)

and **2** (m/z 243), which were present in all the three treatments performed (O_3, PEC and O_3 + PEC), probably due to the capacity of hydroxyl radical to be formed during all the treatments used. The product **3** (m/z 229) was detected in O_3 and O_3 + PEC treatments, indicating that this product can be formed only during the treatment using O_3. The product **4** (m/z 225) was detected in O_3 + PEC and PEC treatments, indicating that the PEC treatment was responsible for this product formation. The product identified as compound **1** was generated by oxidation (MW 330, m/z 329), where oxygen (16 Da) was introduced in the AY1, the position of hydroxylation cannot be completely elucidated only by LC–MS/MS analyses. The following products **2**, **3** and **4** were not completely elucidated even with the MS/MS experiments performed. New experiments are underway to identify the products obtained.

The presence of aliphatic acids and aromatic acids were also investigated. Optimized MRM experiments were carried out owing to the high sensibility found in the LC–MS/MS analyses. The results showed the presence of malonic, fumaric, tartaric and citric acids in O_3 + PEC and PEC treatments. On the other hand, fumaric and citric acids were detected in O_3 treatment. In this sense, it is worth noting that the results showed different degradation routes for the treatments studied (Scheme 1).

Table 3
Summary of all products detected in the degradation studies of AY1 dye.

Compound	t_R/min	Proposed structures	$[M − H]^-$ m/z [b]	Fragment ion (MS/MS) m/z	Treatment detected
Acid Yellow 1	4.08	–	313	233, 296, 173	O_3, PEC, O_3 + PEC
Product 1 [a]	3.65		329	283, 267, 237	O_3, PEC, O_3 + PEC
Product 2	6.90	Not identified	243	170, 156, 147, 80	O_3, PEC, O_3 + PEC
Product 3	1.77	Not identified	229	185, 121, 93, 81	O_3, O_3 + PEC
Product 4	5.29	Not identified	225	161, 117, 80	PEC, O_3 + PEC
Malonic acid	1.85	–	103	59, 41	PEC, O_3 + PEC
Citric acid	1.87	–	191	111, 87	O_3, PEC, O_3 + PEC
Fumaric acid	2.38	–	115	71, 43	O_3, PEC, O_3 + PEC
Tartaric acid	1.62	–	149	87, 73	PEC, O_3 + PEC

[a] Chemical structure with OH in undefined position in the aromatic ring.

[b] Detected in negative mode with $z = 1$.

Other experiments performed using different potential for ionization did not show any product remaining. Furthermore, for all the intermediates analyzed it was also observed that following 60 min of treatment, all the compounds were completely eliminated from the samples. Table 3 summarizes all the products detected.

4. Conclusions

Our findings show for the first time that the combination of photoelectrocatalysis using TiO$_2$NTs electrode and ozonation (O_3 + PEC) is a powerful system capable of promoting a higher degradation and a higher mineralization of organic compounds even operating in high colorful effluents. The main drawback of the photoelectrocatalytic treatment lies in its low rate of compounds degradation in high concentrated effluents which can be successfully circumvented with its combination with ozonation which is efficient in color removal though lacks the ability to mineralize the dye. Photocatalytic ozonation (O_3 + PC) is a well-established technique in the literature, but under an applied voltage (O_3 + PEC) it was possible to reach an almost 2 times higher decolorization rate of AY1 dye, a total mineralization within a much shorter time and lower electrical energy cost. The efficiency of O_3 + PEC treatment is affected by the AY1 initial concentration and pH, though it has been shown to work in a wide range of concentrations and in all the pHs tested. By increasing the ozone flow, it was possible to obtain a total mineralization of 100 ppm AY1 dye in only 30 min and lower energy costs. Thus, the photoelectrocatalytic ozonation is a new approach among the AOPs, which can be a great alternative for the development of efficient and cost-effective methods of water treatment.

Acknowledgements

References

[1] R. Daghrir, P. Drogui, D. Robert, J. Photochem. Photobiol. A: Chem. 238 (2012) 41–52.
[2] H. Zhang, G. Chen, D.W. Bahnemann, J. Mater. Chem. 19 (2009) 5089–5121.
[3] G.G. Bessegato, T.T. Guaraldo, M.V.B. Zanoni, Modern Electrochemical Methods in Nano, Surface and Corrosion Science, in: M. Aliofkhazraei (Ed.), InTech, 2014, pp. 271–319.
[4] C.E. Patrick, F. Giustino, Adv. Funct. Mater. 21 (2011) 4663–4667.
[5] M.V.B. Zanoni, T. Guaraldo, ECS Trans. 50 (2013) 63–70.
[6] M. Ni, M.K.H. Leung, D.Y.C. Leung, K. Sumathy, Renew. Sustain. Energy Rev. 11 (2007) 401–425.
[7] R.A.G. de Oliveira, M.V.B. Zanoni, Electroanalysis 25 (2013) 2507–2514.
[8] T.J. LaTempa, S. Rani, N. Bao, C.A. Grimes, Nanoscale 4 (2012) 2245–2250.
[9] G.G. Bessegato, J.C. Cardoso, M.V.B. Zanoni, Catal. Today 240 (2014) 100–106.
[10] J.C. Cardoso, T.M. Lizier, M.V.B. Zanoni, Appl. Catal. B: Environ. 99 (2010) 96–102.
[11] I. Paramasivam, H. Jha, N. Liu, P. Schmuki, Small 8 (2012) 3073–3103.
[12] J. Georgieva, E. Valova, S. Armyanov, N. Philippidis, I. Poulios, S. Sotiropoulos, J. Hazard. Mater. 211 (2012) 30–46.
[13] T.A. Egerton, J. Chem. Technol. Biotechnol. 86 (2011) 1024–1031.
[14] T.E. Agustina, H.M. Ang, V.K. Vareek, J. Photochem. Photobiol. C: Photochem. Rev. 6 (2005) 264–273.
[15] L. Sánchez, J. Peral, X. Domènech, Appl. Catal. B: Environ. 19 (1998) 59–65.
[16] J. Nawrocki, B. Kasprzyk-Hordern, Appl. Catal. B: Environ. 99 (2010) 27–42.
[17] F. Parrino, G. Camera-Roda, V. Loddo, G. Palmisano, V. Augugliaro, Water Res. 50 (2014) 189–199.
[18] U. Cernigoj, U.L. Stangar, J. Jirkovský, J. Hazard. Mater. 177 (2010) 399–406.
[19] K. Rajeshwar, M.E. Osugi, W. Chanmanee, C.R. Chenthamarakshan, M.V.B. Zanoni, P. Kajitvichyanukul, R. Krishnan-Ayer, J. Photochem. Photobiol. C: Photochem. Rev. 9 (2008) 171–192.
[20] S. Wang, F. Shiraishi, K. Nakano, Chem. Eng. J. 87 (2002) 261–271.
[21] K. Rajeshwar, Encyclopedia of Electrochemistry, in: A.J. Bard, M. Stratmann, S. Licht (Eds.), Wiley-VCH Verlag GmbH & Co., 2007, pp. 1–54.
[22] D. Tomova, V. Iliev, S. Rakovsky, M. Anachkov, A. Eliyas, G.L. Puma, J. Photochem. Photobiol. A: Chem. 231 (2012) 1–8.
[23] Z. Zsilák, E. Szabó-Bárdos, O. Fónagy, O. Horváth, K. Horváth, P. Hajós, Catal. Today 230 (2014) 55–60.
[24] G. Liao, D. Zhu, L. Li, B. Lan, J. Hazard. Mater. 280 (2014) 531–535.
[25] J.R. Bolton, K.G. Bircher, W. Tumas, C.A. Tolman, Pure Appl. Chem. 73 (2001) 627–637.
[26] M. Mehrjouei, S. Müller, D. Möller, Chem. Eng. J. 248 (2014) 184–190.